

Photoelectrochemical activity of electrophoretically deposited zinc oxide coatings on stainless steel substrates

Algimantas Ivanauskas,

Agnė Šulčiūtė,

Eugenijus Valatka*

*Department of Physical Chemistry,
Kaunas University of Technology,
Radvilėnų Rd. 19,
LT-50254 Kaunas,
Lithuania*

Highly photoactive zinc oxide (ZnO) coatings on AISI 304 type stainless steel were formed by electrophoretic deposition using methanol solutions. The prepared coatings were characterized by X-ray diffraction (XRD), Fourier-transform infrared (FTIR) spectroscopy and photovoltammetry analysis. The influence of deposition time and voltage on the amount of immobilized ZnO was experimentally studied. The photoelectrochemical performance of the prepared coatings was evaluated in 0.1 M Na₂SO₄ aqueous solutions containing various concentrations of glycerol. The obtained experimental results show that the highest photoelectrochemical activity is characteristic of the coatings annealed at 573–673 K. It was established that the steady state photocurrent decreases as a concentration of glycerol increases.

Key words: photoelectrochemical activity, electrophoretic deposition, zinc oxide

INTRODUCTION

Zinc oxide (ZnO) is well-known as *n*-type semiconducting material with a band gap of ~3.35 eV. It crystallizes predominantly in the hexagonal wurtzite-type structure. ZnO is characterized by specific optical, electrical and thermal properties that are very attractive for diverse industrial applications (rubber industry, ceramics, plastics, pigments, optoelectronics, etc.) [1–3]. ZnO can be potentially used in photocatalytic processes, such as oxidation of organic compounds or water splitting into hydrogen and oxygen. In order to increase the photocatalytic efficiency of ZnO particles, they can be deposited on electroconductive substrates and biased positively by applying an external voltage. In this way, the rate of photoelectron and hole recombination is significantly reduced; consequently, the rate of surface reactions is increased. It has been shown in numerous papers that ZnO coatings can be prepared by chemical vapour deposition, radio frequency magnetron sputtering, molecular

beam epitaxy, sol-gel and hydrothermal synthesis, electrochemical or electrophoretic deposition [4–11]. The electrophoretic deposition (EPD) is a cost-competitive technique for obtaining highly uniform films with thickness from the nanometer to micrometer scale by changing the applied voltage and deposition time. The main advantages of the EPD method are as follows [12, 13]: it can be applied to any solid available in a form of fine powder, rapid film deposition, low cost, simple instrumentation, little restriction on the shape of substrates, conservation of materials. EPD has been reported to be a very useful technique for the preparation of nanostructured ZnO films [13–25]. Both aqueous and non-aqueous ZnO suspensions have been used for the coating of various substrates (transparent conductive oxide glass, anodic alumina membranes, steel, nickel).

The aim of the current work was to prepare zinc oxide coatings on stainless steel using EPD method and to determine their photoelectrochemical activity in aqueous solutions. This work is relevant to the development of functional materials and methods suitable for photoelectrocatalytic oxidation of organic compounds and water photosplitting.

* Corresponding author. E-mail: eugenijus.valatka@ktu.lt

MATERIALS AND METHODS

ZnO coatings on stainless steel were prepared by electrophoretic deposition (EPD). All substances were chemically or analytically pure commercial reagents. In this work, a commercial ZnO powder (Reachim, Russia) was used of the following composition (wt.%): ZnO, 99; HCl, 0.01; NO_3^- , 0.001; SO_4^{2-} , 0.01; Fe, 0.001; K, 0.005; Ca, 0.01; Na, 0.025; Mn, 0.0005; Cu, 0.001; As, 0.0002; Pb, 0.01; KMnO_4 , 0.01. AISI 304 type stainless steel plates were used as a support. According to the manufacturer, the composition of stainless steel is as follows (wt.%): C, 0.08; Cr, 18–20; Ni, 8–10.5; Mn, 2.0; Si, 1.0; P, 0.045; S, 0.03; Fe, the balance.

The suspension for EPD was prepared by dispersing 2 g of ZnO powder in methanol (purity 99.5%, Lachema, Czech Republic). A homogenous suspension was achieved under vigorous stirring for 10 min. Two stainless steel plates ($50 \times 25 \times 0.5$ mm each) were immersed into the prepared suspension of ZnO. The distance between the anode and the cathode was 2 cm. EPD synthesis was performed under constant voltage (3–30 V) and was controlled using a DC power supply B5-49 (MNIPI Inc., Russia). The formation of ZnO coatings took place on the cathode. The deposition time was varied from 2 to 15 min. In order to achieve better adhesion of ZnO particles on stainless steel substrate, all samples were thermally treated at 473–873 K for 1 hour under air atmosphere. Some ZnO coatings were peeled off from the substrate for the determination of their structure by X-ray diffraction and infrared absorption spectroscopy.

The X-ray powder diffraction (XRD) data were collected with a DRON-6 (Bourestnik Inc., Russia) powder diffractometer with Bragg-Brentano geometry using Ni-filtered CuK_α radiation and a graphite monochromator. The crystallite size D_{hkl} was calculated from the line broadening using the Scherrer's equation [26]:

$$D_{hkl} = \frac{k \cdot \lambda}{B_{hkl} \cdot \cos \Theta}$$

where λ is the wavelength of the CuK_α radiation (1.54056×10^{-10} m), Θ is the Bragg diffraction angle, B_{hkl} is the full width at the half maximum intensity of the characteristic reflection peak ($2\Theta = 31.66, 34.38, 36.26^\circ$) and k is a constant (the value used in this study was 0.94).

Fourier-transform infrared (FTIR) spectra were measured in the range of $400\text{--}4000\text{ cm}^{-1}$ on a Perkin Elmer FT-IR System infrared spectrometer using KBr pellets (1 mg of the substance was mixed with 200 mg of KBr).

The photoelectrochemical activity of ZnO coatings was investigated by photovoltammetry. The electrochemical measurements in the dark and under UV irradiation were performed with a computer-controlled Autolab PGSTAT12 (Ecochemie, the Netherlands) potentiostat/galvanostat. The GPES[®] 4.9 software was used for the collection and treatment of the experimental data. 0.1 M Na_2SO_4 (purity >99%, Reachim, Russia) solution was used as a supporting elec-

trolyte. The photoactivity of the prepared coatings was also tested by oxidation of glycerol as a model organic compound ($\text{C}_3\text{H}_8\text{O}_3$, purity >99%, Lachema, Czech Republic). The volume of the electrolyte in a photoelectrochemical quartz cell was 100 mL. ZnO coating on the steel substrate was used as a working electrode. $\text{Ag, AgCl} \mid \text{KCl}_{(\text{sat})}$ and a platinum wire were used as the reference and counter electrodes, respectively. The back side of the working electrode was insulated with epoxy resin in order to eliminate its contribution to the dark current. The coated area of the electrode was carefully positioned in the path of the UV irradiation. A General Electric F8W / BLB lamp ($\lambda_{\text{max}} = 366$ nm) was placed at a distance of 2 cm from the ZnO electrode and was used as an UV radiation source. The average power density at 366 nm was determined to be 1.8 mW/cm^2 . The incident photon-to-current efficiency (IPCE) value was calculated by using the following expression [27]:

$$\text{IPCE}(\%) = 100 \frac{1240 \cdot i_{ph}}{\lambda P}$$

where i_{ph} is the photocurrent density in mA/cm^2 , λ is the wavelength of the incident light in nanometers (the value used in this study was 366 nm), P is the incident light intensity in mW/cm^2 .

RESULTS AND DISCUSSION

Synthesis and structural characterization of ZnO coatings

Fig. 1 shows the experimental results of deposited ZnO weight at various voltages as a function of electrophoresis time. It is seen that the amount of deposited ZnO increases almost linearly with the increase in deposition time. Moreover, the rate of ZnO deposit formation increases together with the increase in applied voltages. However, it is well documented [28] that quick formation of particulate coat-

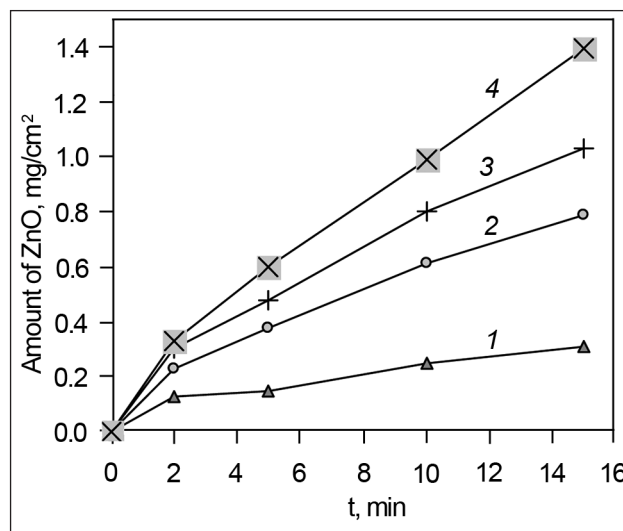


Fig. 1. The amount of immobilized ZnO as a function of electrophoretic deposition time t at different voltages (V): 1 – 3; 2 – 10; 3 – 15; 4 – 30

ings on the electrode can result in poorer deposit quality as an accumulation rate of the particles greatly influences their packing behaviour in coatings. In our case, the most uniform and mechanically stable coatings were obtained after 5 minutes of electrophoresis when the applied potential between electrodes was 10 V. Under such conditions, the amount of deposited ZnO is 0.39 mg/cm². Assuming that the density of ZnO is 5.60 g/cm³, the estimated thickness of the coating is ~0.70 μm.

X-ray diffraction analysis revealed the characteristic diffraction peaks ($2\theta = 31.66, 34.38$ and 36.26°) corresponding to the well-crystallized hexagonal wurtzite ZnO (Fig. 2). According to the Scherrer's equation [26], the average ZnO

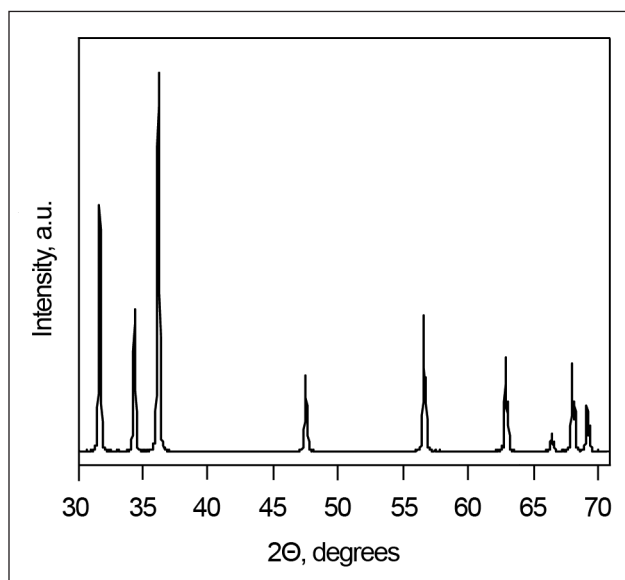


Fig. 2. XRD pattern of zinc oxide annealed at 673 K

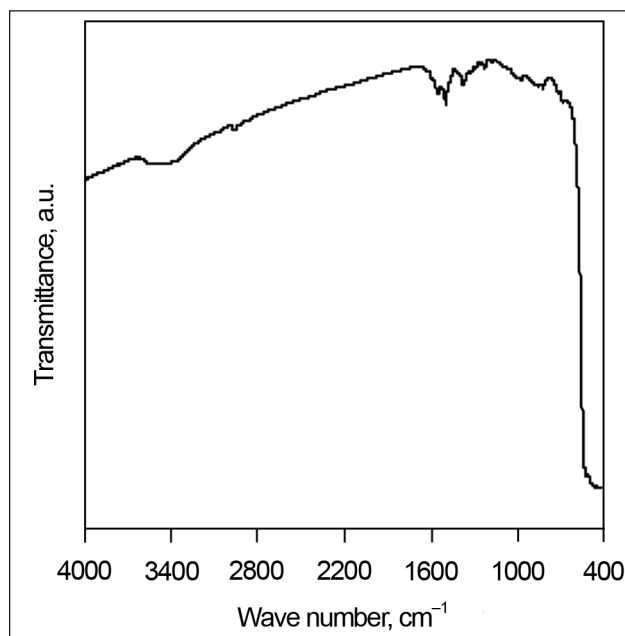


Fig. 3. FTIR pattern of zinc oxide annealed at 673 K

crystallite size was calculated to be 51 nm. The infrared absorption spectrum (Fig. 3) showed a large absorption band centered at 3447 cm^{-1} , that can be assigned to the stretch vibrations of hydroxy groups. The peaks observed at $1589, 1340$ and 673 cm^{-1} can be attributed to the impurities derived from the industrial production of zinc oxide. A broad band centered at 495 cm^{-1} corresponds to the characteristic stretching frequency of Zn-O bond and it can be used for the identification of zinc white pigment in the IR spectra of real paint sample layers [29].

Photoelectrochemical characterization of ZnO coatings

The photoelectrochemical behaviour of ZnO electrode was determined from the current-potential curves obtained in 0.1 M Na₂SO₄ solutions both in the dark and under UV irradiation (Fig. 4). The potential was swept from -0.5 V to $+1.0\text{ V}$ at 5 mV/s scan rate. It is seen that the UV irradiation caused a significant increase in the observed currents. Such behaviour is characteristic of n-type semiconducting materials and is related to photogenerated electrons diffusion through the catalyst film towards the cathode [30]. The observed anodic photocurrent can be related to the generation of hydroxyl radicals ($\cdot\text{OH}$) and other oxidation products (e. g., H₂O₂) at the surface of ZnO electrodes [31]. The presence of $\cdot\text{OH}$ radicals at the interface of ZnO / aqueous solution was confirmed by radical-trapping technique. Hydrogen peroxide is formed as a result of the interaction of generated hydroxyl radicals. The rate of hydrogen peroxide formation in aerated ZnO aqueous suspensions is highly dependent on the presence of various organic and inorganic species [32]. It should be emphasized that at the same time the photodissolution (photocorrosion) of ZnO can take place to some extent due to the self-oxidation through photohole generation [33].

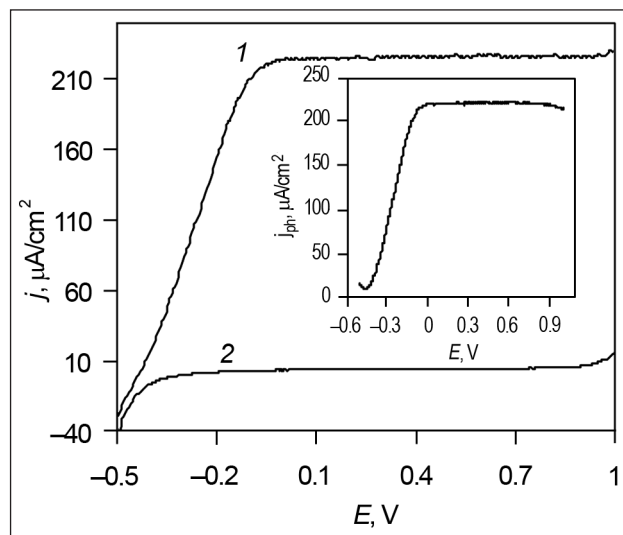


Fig. 4. Characteristic voltammograms of ZnO electrode under UV irradiation (1) and in the dark (2) recorded at 5 mV/s potential scan rate in 0.1 M Na₂SO₄ electrolyte at 291 K. Inset: plot of the photocurrent density j_{ph} with respect to the applied potential E

In order to suppress the rate of ZnO photocorrosion and to enhance its photocatalytic performance, the various methods are under investigation [34–37].

The results presented in the inset of Fig. 4 show that the photocurrent reaches a limiting value at $E > 0$ V. This limiting photocurrent is influenced by various factors, such as the structure of the catalyst, particle size and shape, the electrical conductivity [30, 31]. It is well established that a depletion layer can be developed in continuous semiconductor films upon their contact with the electrolyte. The depletion layer facilitates the separation of generated photoelectrons and photoholes. As a result, the overall efficiency of photoelectrochemical processes increases. Based on the Butler-Gartner model and taking into account the fact that the rising part of the photovoltammograms is linear (Fig. 4), it can be inferred that the depletion layer is formed in the prepared ZnO films. The increase in currents recorded at more positive than +0.9 V potential bias may be associated with stainless steel dissolution and oxygen evolution [38]. The observed photocurrents tend slightly to decrease in this potential range (the inset of Fig. 4).

The experimental results showed that the value of generated photocurrent depends on electrode preparation conditions (Fig. 5). ZnO electrodes annealed at 573–673 K are characterized by the highest photoactivity. The annealing at higher temperatures (>673 K) results in the decrease of photocurrents. This may be associated with thermal diffusion of some ions (Fe^{3+} , Cr^{3+} , Ni^{2+}) from stainless steel to the ZnO layer and the contamination of photocatalyst. Based on the photocurrent measurements, the maximum value of incident photon-to-current efficiency (IPCE) for ZnO photoelectrodes was calculated to be 43.4%.

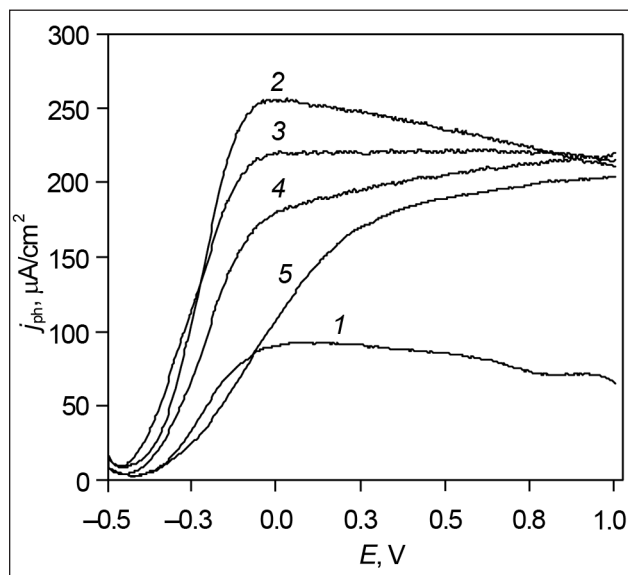


Fig. 5. Plot of the photocurrent density j_{ph} with respect to the applied potential E for ZnO electrode annealed at different temperatures (K): 1 – 473, 2 – 573, 3 – 673, 4 – 773, 5 – 873. Potential scan rate $v = 5$ mV/s, 0.1 M Na_2SO_4 electrolyte at 291 K

It has been found that the UV irradiation has a significant impact on the value of open circuit potential (Fig. 6). In the dark, the ZnO electrode has a potential in the range of -0.23 – -0.3 V depending on electrode preparation conditions. Under UV irradiation, the potential decreases approximately to -0.4 V. When the light is switched off, the potential of ZnO electrode increases and reaches its initial value. The observed decrease in the potential can be explained by the fact that the photoholes react rapidly with water molecules, while the photoelectrons are accumulating on the surface of ZnO particles and charging them negatively. Chronoamperometry studies confirmed that ZnO coatings are very active under UV irradiation (Fig. 7).

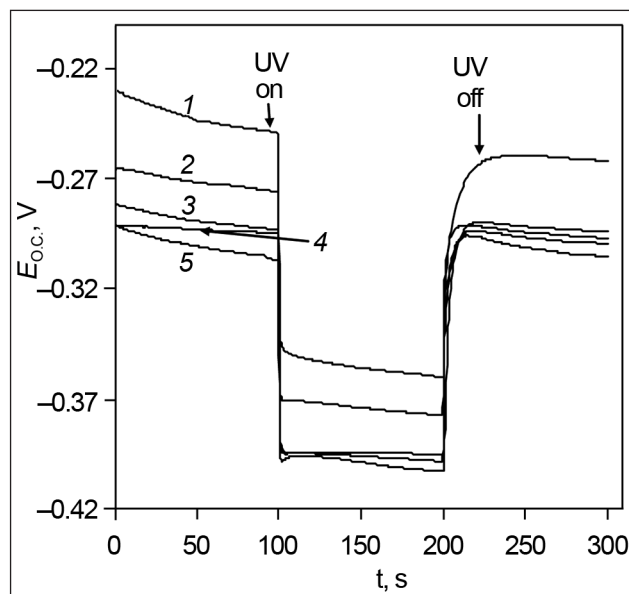


Fig. 6. Variation of the open circuit potential E_{oc} of ZnO electrode annealed at different temperatures (K): 1 – 473, 2 – 573, 3 – 773, 4 – 873, 5 – 673

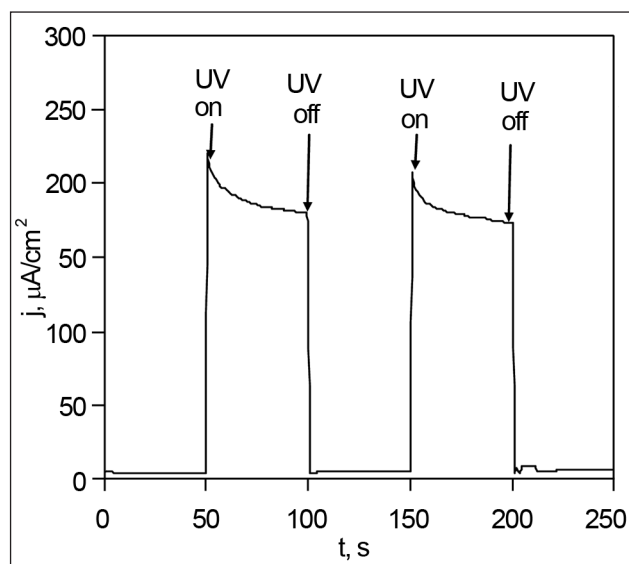


Fig. 7. Chronoamperometric curves of ZnO electrode in the dark and under UV irradiation at +0.6 V potential in 0.1 M Na_2SO_4 electrolyte

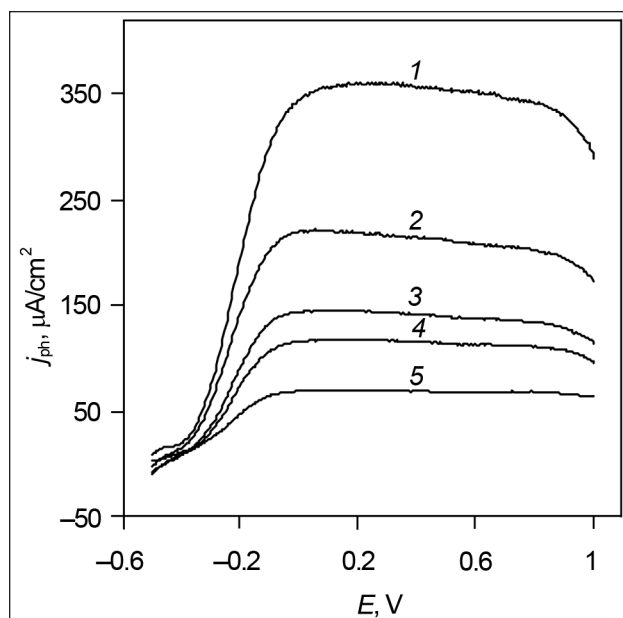


Fig. 8. Plot of the photocurrent density j_{ph} with respect to the applied potential E in 0.1 M Na_2SO_4 electrolyte containing various glycerol concentrations (mM): 1–1, 2–2, 3–3, 4–5, 5–10. Potential scan rate $v = 5$ mV/s

Fig. 8 shows the photocurrent-potential curves for the ZnO electrode in 0.1 M Na_2SO_4 supporting electrolyte in the presence of glycerol at various concentrations. It is seen that the photocurrents increase steeply with the applied bias at low potentials (< -0.3 V) and then reach a saturation at more positive potentials. The photocurrent saturation can be explained by assuming that the rate of electron transfer in the ZnO film is comparable to the rate of photohole capture at the ZnO/solution interface. The latter is influenced by the availability of electron donors at the particle surface, their nature and interaction with the ZnO surface [39, 40]. The data presented in Fig. 8 show that the observed photocurrents significantly increased in the presence of 1 mM of glycerol. However, a further increase in glycerol concentration results in the decrease of the generated photocurrents. A similar dependence of photocurrent on the initial concentration of organic additives was found in the case of methylene blue and phenol using TiO_2 or WO_3 electrodes [41, 42]. The decrease in photocurrents can be related to the formation of intermediates on the surface of ZnO particles. These compounds can act as photohole/photoelectron recombination centres and reduce the overall efficiency of photoelectrochemical processes. It is known [43] that the main intermediates of glycerol photocatalytic oxidation are glyceraldehyde and 1,3-dihydroxyacetone.

CONCLUSIONS

Zinc oxide coatings on AISI 304 type stainless steel were prepared by electrophoretic deposition and characterized by X-ray diffraction, infrared absorption and photovoltammetry analysis. The obtained experimental results show that

the amount of ZnO deposited on steel is dependent on the electrophoresis time and applied voltage. The optimum conditions for the synthesis of uniform and mechanically stable coatings were found to be 10 V potential and 5 min of deposition. Under such conditions, the amount of immobilized ZnO is 0.3–0.4 mg/cm^2 . XRD analysis confirmed that the zinc oxide consists of the hexagonal (wurtzite) phase, the average crystallite size being about 51 nm. The prepared coatings were found to be highly photoactive under UV exposure in 0.1 M Na_2SO_4 electrolyte. The highest photocurrent density is obtained for the coatings annealed at 673 K and containing about 0.39 mg/cm^2 of ZnO. The oxidation of glycerol was used as a test reaction in order to evaluate the photoelectrocatalytic activity of the prepared coatings. It was found that the generated photocurrent increases when a small amount (1 mM) of glycerol is added to the supporting electrolyte. A further increase in the concentration of glycerol leads to the decrease in the observed photocurrents.

Received 20 November 2012

Accepted 5 February 2013

References

1. C. Klingshirn, *Chem. Phys. Chem.*, **8**, 782 (2007).
2. Ü. Özgür, I. Alivov, C. Liu, et al., *J. Appl. Phys.*, **98**, 103 (2005).
3. A. Moezzi, A. M. McDonagh, M. B. Cortie, *Chem. Eng. J.*, **185–186**, 1 (2012).
4. J. Cheng, R. Guo, Q. M. Wand, *Appl. Phys. Lett.*, **85**, 5140 (2004).
5. O. A. Fouad, A. A. Ismail, Z. I. Zaki, R. M. Mohamed, *Appl. Catal., B*, **62**, 144 (2006).
6. T. M. Barnes, J. Leaf, C. Fry, C. A. Wolden, *J. Cryst. Growth*, **274**, 412 (2005).
7. J. H. Lee, K. H. Ko, B. O. Park, *J. Cryst. Growth*, **247**, 119 (2005).
8. A. E. Morales, M. H. Zaldivar, U. Pal, *Opt. Mater.*, **29**, 100 (2006).
9. Z. Yan, Z. T. Song, W. L. Liu, Q. Wan, F. M. Zhang, S. L. Feng, *Thin Solid Films*, **492**, 203 (2005).
10. H. Y. Kim, J. H. Kim, M. O. Park, S. Im, *Thin Solid Films*, **398**, 93 (2001).
11. A. J. C. Fiddes, K. Durose, A. W. Brinkman, J. Woods, P. D. Coates, A. J. Banister, *J. Cryst. Growth*, **159**, 210 (1996).
12. I. Corni, M. P. Ryan, A. R. Boccaccini, *J. Eur. Ceram. Soc.*, **28**, 1353 (2008).
13. Y. Hara, J. R. S. Brownson, M. A. Anderson, *Int. J. Appl. Ceram. Technol.*, **12**, 115 (2012).
14. E. M. Wong, P. C. Searson, *Chem. Mater.*, **11**, 1959 (1999).
15. F. Tang, Y. Sakka, T. Uchikoshi, *Mater. Res. Bull.*, **38**, 207 (2003).
16. F. Tang, T. Uchikoshi, Y. Sakka, *J. Am. Ceram. Soc.*, **85**, 2161 (2002).
17. Y. Wang, I. Leu, M. Hon, *J. Cryst. Growth*, **237**, 564 (2002).
18. Y. Wang, I. Leu, M. Hon, *J. Mater. Chem.*, **12**, 2439 (2002).

19. K. Wu, I. Zhitomirsky, *Int. J. Appl. Ceram. Technol.*, **8**, 920 (2011).
20. H. Chen, C. Lin, Y. Lai, et al., *J. Power Sources*, **196**, 4859 (2011).
21. X. Yin, X. Liu, L. Wang, B. Liu, *Electrochem. Commun.*, **12**, 1241 (2010).
22. L. Miao, S. Cai, Z. Xiao, *J. Alloys Compd.*, **490**, 422 (2010).
23. J. Lee, I. Leu, Y. Chung, M. Hon, *Nanotechnology*, **17**, 4445 (2006).
24. M. Verde, A. C. Caballero, Y. Iglesias, M. Villegas, B. Ferrari, *J. Electrochem. Soc.*, **157**, H55 (2010).
25. M. Verde, M. Peiteado, A. C. Caballero, M. Villegas, B. Ferrari, *J. Colloid Interface Sci.*, **373**, 27 (2012).
26. L. V. Azaroff, *Elements of X-ray Crystallography*, Mc Graw Hill Book Co, New York (1968).
27. J. Georgieva, S. Armyanov, E. Valova, I. Puolios, S. Sotiropoulos, *Electrochem. Commun.*, **9**, 365 (2007).
28. L. Besra, M. Liu, *Prog. Mater. Sci.*, **52**, 1 (2007).
29. S. Vahur, A. Teearu, I. Leito, *Spectrochim. Acta, Part A*, **75**, 1061 (2010).
30. K. Rajeshwar, in: A. J. Bard, M. Stratmann, S. Licht (eds.), *Encyclopedia of Electrochemistry*, Vol. 6, Wiley-VCH, Weinheim, Germany (2002).
31. M. Gratzel, *Heterogeneous Photochemical Electron Transfer*, CRC Press, Boca Raton (1989).
32. X. Domenech, J. A. Ayllon, J. Peral, *Environ. Sci. Pollut. R.*, **8**, 285 (2001).
33. P. Spathis, I. Poullos, *Corros. Sci.*, **37**, 673 (1995).
34. L. R. Zheng, Y. H. Zheng, C. Q. Chen, Y. Y. Zhang, X. Y. Lin, Q. Zheng, K. M. Wei, *ChemPlusChem*, **77**, 217 (2012).
35. S. L. Xie, X. H. Lu, T. Zhai, W. Li, M. H. Yu, C. L. Liang, Y. X. Tong, *J. Mater. Chem.*, **22**, 14272 (2012).
36. L. W. Zhang, H. Y. Cheng, R. L. Zong, Y. F. Zhu, *J. Phys. Chem. C*, **113**, 2368 (2009).
37. H. B. Fu, T. G. Xu, S. B. Zhu, Y. F. Zhu, *Environ. Sci. Technol.*, **42**, 8064 (2008).
38. I. Betova, M. Bojinov, T. Laitinen, K. Makela, P. Pohjanne, T. Saario, *Corros. Sci.*, **44**, 2675 (2002).
39. D. Jiang, H. Zhao, S. Zhang, R. John, *J. Photochem. Photobiol., A*, **177**, 253 (2006).
40. J. Georgieva, S. Armyanov, E. Valova, I. Poullos, S. Sotiropoulos, *Electrochim. Acta*, **51**, 2076 (2006).
41. Ž. Kulėšius, E. Valatka, *J. Appl. Electrochem.*, **37**, 415 (2007).
42. S. Ostachavičiūtė, J. Baltrušaitis, E. Valatka, *J. Appl. Electrochem.*, **40**, 1337 (2010).
43. V. Maurino, A. Bedini, M. Minella, F. Rubertelli, E. Pelizzetti, C. Minero, *J. Adv. Oxid. Technol.*, **11**, 184 (2008).

Algimantas Ivanauskas, Agnė Šulčiūtė, Eugenijus Valatka

ELEKTROFOREZĖS METODU NUSODINTŲ CINKO OKSIDO DANGŲ ANT NERŪDIJANČIO PLIENO FOTOELEKTROCHEMINIS AKTYVUMAS

Santrauka

Taikant elektroforezės metodą suformuotos cinko oksido (ZnO) dangos ant AISI 304 markės nerūdijančio plieno ir ištirtas jų fotoelektrocheminis aktyvumas Na₂SO₄ vandeniniuose tirpaluose. Nustatyta, kad mechaniškai stabiliausias ir tolygiausias dangos gaunamos, kai sintezės metu taikoma 10 V įtampa tarp elektrodų, trukmė – 5 min., o nusodinto cinko oksido kiekis – 0,3–0,4 mg/cm². Rentgeno spindulių difrakcinės analizės rezultatai patvirtino, kad dangos sudarytos iš viurcito fazės cinko oksido, kurio kristalitų vidutinis dydis yra 51 nm. Fotovoltamperometrijos metodu nustatyta, kad gautosios dangos yra labai aktyvios veikiant UV spinduliuotei, o didžiausią fotosrovę 0,1 mol/l Na₂SO₄ tirpale generuoja 673 K temperatūroje iškaitintos dangos. Ištyrus dangų fotoelektrocheminį aktyvumą glicerolio atžvilgiu, nustatyta, kad nedidelis jo priedas (1 mmol/l) padidina stebimąsias fotosroves, tačiau didesnių koncentracijų sąlygomis užfiksuotas fotosrovės verčių mažėjimas.